Contactless Charging Systems

Tomio Yasuda*, Isami Norigoe*, Shigeru Abe**,Yasuyoshi Kaneko**
*Technova Inc., Tokyo, Japan
**Saitama University, Saitama, Japan
E-mail: yasuda@technova.co.jp

Two technologies have greatly accelerated the practical use of contactless charging systems: the contactless power transformer achieved a compact size and good tolerance to misalignment by improving the core architecture, while the charging controller raised effectiveness and lowered noise with a new DC/DC converter. Specifically, the new DC/DC converter can operate buck-boost and soft-switching. A bench test and PHEV test confirmed that a contactless charging system composed of these new technologies charged stably despite gap changes and misalignment.

Keywords: ***contactless power transfer system, inductive power transfer***

I. INTRODUCTION

Plug-in hybrid electric vehicles (PHVs) and electric vehicles (EVs) are being developed and commercialized, due to environmental concerns and rising oil prices. PHVs and EVs require connection to a power supply by electric cables for battery charging. A contactless power transfer system (Fig. 1) would have many advantages, including the convenience of being cordless and safety during high-power charging. A contactless power transfer system for electric vehicles must have high efficiency, a large air gap and good tolerance to misalignment in the lateral direction, and be compact and lightweight. Transformers with circular cores and single-sided windings have commonly been used [1, 2]; however, we have revealed that a transformer with rectangular cores and double-sided winding has many advantages for good tolerance to misalignment in the lateral direction and is compact and lightweight [3, 4, 5, 6]. Professor Boys and his research team of Auckland University have presented that the weak point of a transformer with circular cores and single-sided windings for electric vehicles is tolerance to misalignment [2], and they have developed a transformer with double-sided winding named Flux Pipe to solve this weak point [7, 8]. It is expected that a transformer with double-sided winding for electric vehicles will become a main type.

Here, the authors introduce a new transformer with H-shaped core, which is more efficient, more robust to misalignment and lighter than previous rectangular core.

The test results of the transformer with H-shaped core and the new **DC/DC converter** are described.

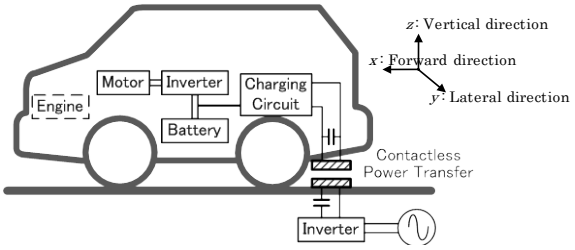

Fig.1. Contactless power transfer system for an EV.

II. CONTACTLESS CHARGING SYSTEM

A. Contactless charging system

Figure 2 shows a schematic diagram of the contactless charging system composed of the contactless power transferring part and the charging controller of the battery part. The contactless power transferring part adopts the series capacitor for primary winding and the parallel resonant capacitor for the secondary winding. A full-bridge inverter is used as a high-frequency power supply. The cores are made of ferrite and the windings are litz wires. The charging controller part adopts double voltage rectifier circuit and the charging control. A double voltage rectification is used as a rectifying circuit. Critical mode fly backing interleave DC/DC converter is used as a charging control.

B. Equivalent circuit of contactless power transfer

Figure 3 shows a detailed equivalent circuit, which consists of a T-shaped equivalent circuit to which resonant

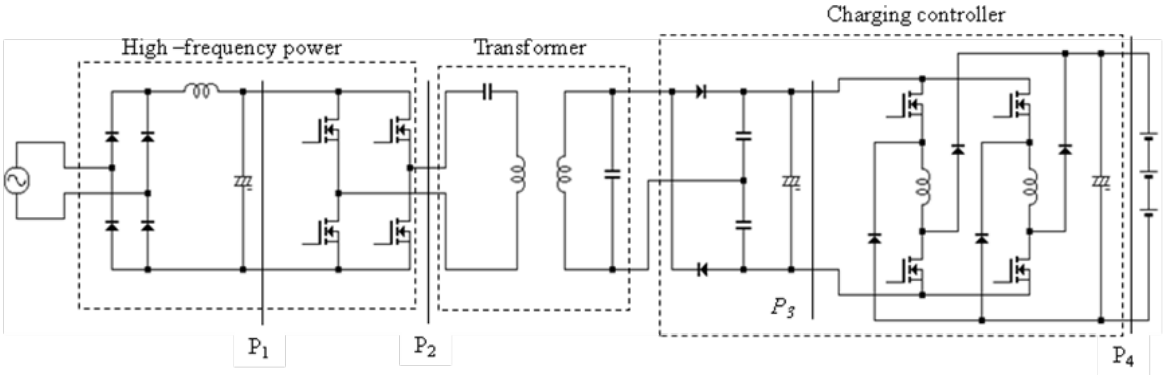

Fig.2. Contactless charging system

capacitors C_S and C_P and a resistance load R_L have been added. Primary values are converted into secondary equivalent values using the turn ratio $a = N_1/N_2$ (primes are used to indicate converted values).

When the ferrite core and the litz wire are used, r_0 shows the iron loss, winding resistance r_1, and r_2 are very small compared with reactance x_0 of the transformer, x_1, and x_2 in the power supply frequency. Therefore, the analysis is advanced with the circuit that omits winding resistance r_1, r_2, and iron loss r_0. Moreover, the secondary rectifying circuit and the smoothing capacitor are omitted and the circuit connects only C_P and resistance load R_L .

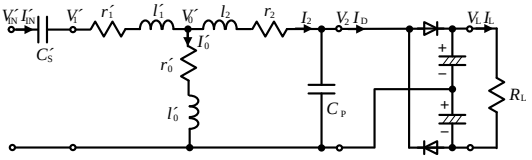

Fig.3. Detailed equivalent circuit of ontactless power transfersy stems.

C. *Series and parallel resonance capacitor*

To achieve resonance with the self-reactance of the secondary winding $\omega_0 L_2$, which is equivalent to adding a mutual reactance x'_0 and a leakage reactance x_2, the secondary parallel capacitor C_P is given by:

$$\frac{1}{\omega_0 C_P} = \omega_0 L_2 = x_p = x'_0 + x_2 \tag{1}$$

The primary series capacitor C_S (C'_S denotes its secondary equivalent) is determined as:

$$\frac{1}{\omega_0 C'_S} = x'_s = \frac{x'_0 x_2}{x'_0 + x_2} + x'_1 \tag{2}$$

D. *Ideal transformer characteristics*

The input voltage V'_{IN} and the input current I'_{IN} can be expressed as follows in (3).

$$V'_{IN} = bV_2 = b\,V_L, \quad I'_{IN} = I_L/b, \quad b = \frac{x'_0}{x'_0 + x_2}. \tag{3}$$

This equation represents the equivalent circuit of a transformer with these capacitors, which is the same as an ideal transformer with a turn ratio of b at the resonant frequency.

Without a rectifier circuit, the efficiency is approximated from the expression (4).

$$\eta = \frac{R_L I_L^2}{R_L I_L^2 + r'_1 I'^2_1 + r_2 I_2^2} = \frac{R_L}{R_L + \frac{r'_1}{b^2} + r_2\left\{1 + \left(\frac{R_L}{x_P}\right)^2\right\}} \tag{4}$$

The maximum efficiency η_{max} is obtained when $R_L = R_{Lmax}$.

$$\eta_{max} = \frac{1}{1 + \frac{2r_2}{x_P}\sqrt{\frac{1}{b^2}\frac{r'_1}{r_2} + 1}} \qquad R_{Lmax} = x_P\sqrt{\frac{1}{b^2}\frac{r'_1}{r_2} + 1} \tag{5}$$

III. NEW CORE ARCHITECTURE POWER TRANSFORMER

A. *Rectangular core type and H-shaped core type transformer*

A transformer with rectangular cores and double-sided winding has many advantages for good tolerance to misalignment and compact and lightweight. We developed some transformers with rectangular cores [5]. Figure 4 (a) shows a 1.5kW transformer for EVs and its characteristics are presented in [5, 6]. The gap length and misalignment characteristics of this transformer depend on size of the magnetic poles and windings. Even if the width of the windings is reduced, ampere turns do not change in the same number of turns. So, we designed a transformer with H-shaped cores that has same length of the ferrite cores and same turns of the windings, and that consists of wide

exposed magnetic poles and narrow windings coil as shown in Fig. 4 (b).

The following effects can be expected of the transformer with H-shaped cores:

- Reducing weight by decreasing length of windings and volume of ferrite.
- Reducing copper loss of the transformer by decreasing length of windings.
- More tolerance to misalignment in the lateral direction by increasing the width of exposed magnetic poles.

Table I lists the design goal of a transformer with H-shaped cores. The misalignment of the forward direction is easily limited by the use of a wheel stopper, which helps drivers to position the forward direction of the PHEV/EV for charging.

Table II lists the specifications of both transformers with H-shaped cores and rectangular cores. Figure 4 shows the photographs and size of these transformers. The weight of a transformer with H-shaped cores is 3.9kg which is lighter than that with rectangular cores (4.6kg). The weight of the winding part in a transformer with H-shaped cores is 2.0kg, lighter than that with rectangular cores (2.9kg).

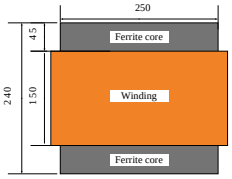

(a) Transformer with rectangular cores.

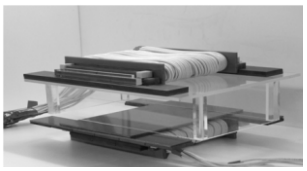

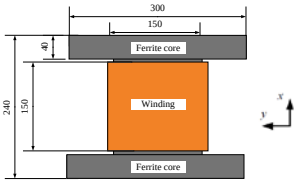

(b) Transformer with H-shaped cores.

Fig.4. Transformer`s outline and their dimensions.

TABLE I. DESIGN GOAL

Rated power		1.5kW
Weight		4.0kg
Gap length		70±30mm
Tolerance to Misalignment	*x*	±45mm
	y	±150mm

TABLE II. SPECIFICATION

Type		Rectangular core	H-shaped core
Core		FDK6H20	FDK6H20,TDKPC40
Litz wire		φ0.25mm×384	φ0.1mm×800
Weight of the Secondary		4.6kg	3.9kg
Size		240×250×40mm	240×300×40mm
Winding	Primary	18T×1P	20T×3P
	Secondary	9T×2P	6T×9P
Aluminum sheet		400×600×1mm	

B. *Characteristics of normal position*

Table III lists the experimental results at the normal position (mechanical gap length of 70mm) of the transformer with H-shaped cores. The efficiency η ($=P_3/P_2$) of the transformer with rectangular cores was higher than that with H-shaped cores in Table III because the gap length with the transformer covers was different. The efficiency of the transformer with rectangular cores became 94.6% when the gap length with the transformer covers was the same 70mm, and the efficiency of the transformer with H-shaped cores of 94.9% was higher than that with rectangular cores.

TABLE III. EXPERIMENTAL RESULT OF NORMAL POSITION.

Type	Rectangular core			H-shaped core			
Fo[kHz]	20			30			
Gap[mm]	70			70			
X[mm]	0	45	0	0	45	0	0*
Y[mm]	0	0	150	0	0	150	0
Pout[W]	1489	1166	1528	1507	1503	1506	3060
H[%]	95.3	91.9	93.1	94.9	93.7	93.0	94.7
Cs/Cp[μF]	0.696/2.30			0.189/1.91			

*Value with 3kW feeding power

C. *Characteristics with Change in gap length and positions*

Figure 5 shows the characteristics of the transformer

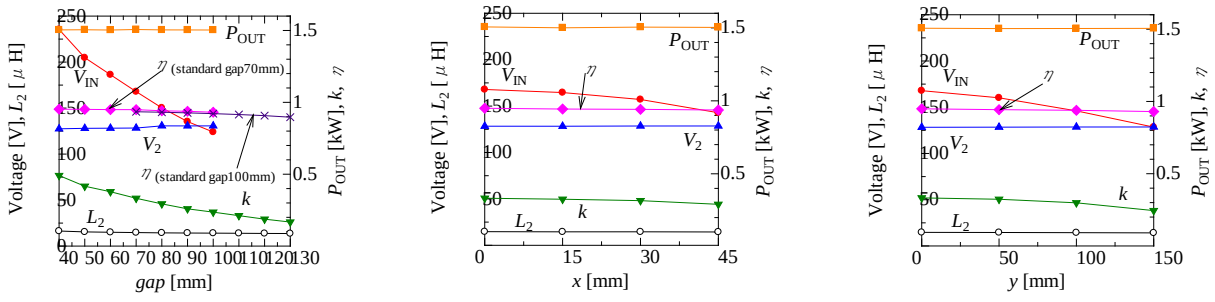

Fig. 5. Experimental result of gap change and misalignment.

with H-shaped cores when the gap length or position is changed. The misalignment directions are shown in Fig. 4. The coupling factor k was decreased when the gap length or misalignment was increased because the magnetic reluctance of the main flux path became larger. The secondary self-inductance L_2 was almost constant. As the values of the parallel capacitors Cp are determined by (1), the values of the resonant capacitors Cs and Cp remained constant during the experiment.

The coupling factor k and ideal transformer turn ratio b decreased when the gap length became larger; therefore, the voltage ratio (V_2 / V_{IN}) increased, as indicated by (3). The input voltage V_{IN} was adjusted to give an output power P_{OUT} of 1.5 kW. V_{IN} and V_2 roughly satisfied the relation of (3) though the gap length changed. The efficiency η decreased from 95.2% to 93.1% when the gap length increased from 40mm to 100mm. The average value of efficiency was 94.5%.

The efficiency η of the transformer with rectangular cores and H-shaped cores were 93.1% and 93.0% respectively at maximum misalignment in the lateral direction y. The reduced efficiency of the transformer with H-shaped cores compared with efficiency of the normal position was 1.9%, and was smaller than the 2.2% of that with rectangular cores. The transformer with H-shaped cores acquired good tolerance to misalignment in the lateral direction by increasing the length of magnetic poles.

D. *Characteristics with a wide gap*

The characteristics of the transformer with a wide gap are of particular interest with respect to practical application of the transformer for contactless power transfer. The minimum ground clearance for PHVs and EVs is approximately 140mm. The gap length was 100mm when the primary side transformer of 40mm in thickness was put directly on the ground in the parking lot. The characteristics of a transformer with standard gap length of 100mm were measured. The values of the resonant capacitors C_S and C_P were still decided by the parameters of the transformer with standard gap length of 100mm. The input voltage V_{IN} was adjusted to give an output power P_{OUT} of 1.5 kW. The coupling factor k and the input voltage V_{IN} were decreased when the gap length became larger, as shown in Fig. 7. The efficiency η decreased from 93.5% to 92.1% to 89.7% when the gap length increased from 70mm to 100mm to 130mm, respectively.

Although the average value of the efficiency decreased to 91.9%, it is possible to transfer 1.5 kW even at a gap length of 100mm ±30mm.

E. *Temperature rise test*

The full charging time of 1.5kW with AC 100V is assumed to be about 4 hours and 10 hours or more, for PHVs and EVs, respectively. Therefore, the temperature rise of the core and the winding of the transformer with H-shaped cores become more important because this size can be smaller than that of the circular cores with a single-sided winding transformer. Figure 9 shows the result of the temperature rise test for the transformer with H-shaped cores. The temperature of the secondary core and winding became the highest but were saturated 3 hours later because of thermal equilibrium. It was confirmed to transfer for 8 hours or more because this temperature is much lower than the Curie temperature of the ferrite and the kindling temperature for the composition material of the transformer. The efficiency η has improved by about 1.0% compared with the beginning of the experiment because the loss of the ferrite has decreased with the temperature rise.

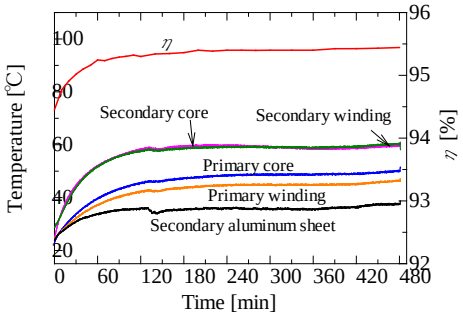

Fig. 6. Temperature rise test.

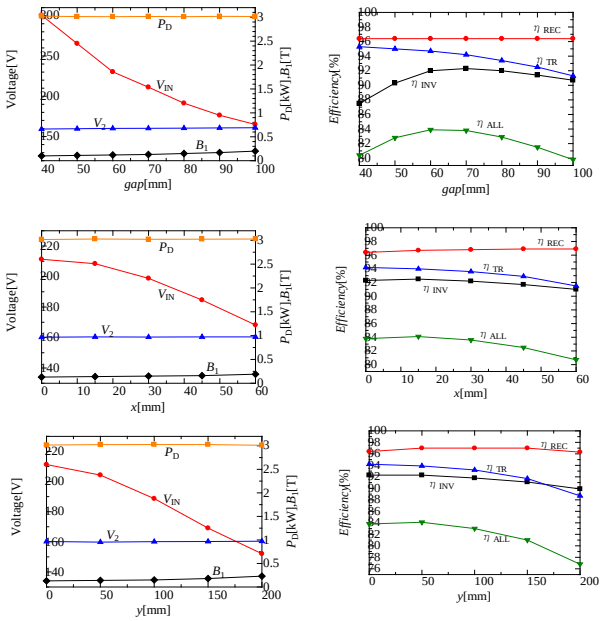

Fig. 7. Experimental result of gap change and misalignment.

F. Characteristics of 3kW power transfer

The 3kW charging with AC200V can decrease the charging time about half compared to 1.5kW charging with AC100V. As the current density of the winding and the flux density in the core are not high, the 3kW transfer test was performed by using the proposed 1.5kW transformer with H-shaped cores. The efficiency η at normal position was 94.7%, as shown in Table III. Figure 7 shows the characteristics of the transformer when the gap length or position is changed. This proposed transformer was able to transfer the power of 3kW by the average efficiency 93% or more.

VI. CHARGE CONTROLLOR

A. Circuit of the charge controller

The charge controller is composed of the rectifier circuit and the charging control. A double voltage rectifier circuit is used for high efficiency.

Critical mode fly backing interleave DC/DC converter is used for high efficiency and low noise. The DC/DC converter performs buck-boost for the change of the secondary voltage by the gap length change and positions change.

The converter is controlled constant current charging and constant voltage charging. The control instruction values are set by the CAN communication. Table IV shows the specifications of the developed DC/DC converter.

Figure 8 shows the waveform of the developed critical mode fly backing interleave DC/DC converter. Duty ratio of the converter is controlled 0.1~0.9 and the frequency of the converter is controlled 40kHz~140kHz.

TABLE IV. Specifications of DC/DC Convertor.

Type	Critical Mode Fly-back Interleave DC/DC Convertor
Input voltage	100～400V
Output voltage	200～300V
Output Current	Max 7.5A
Control	Constant Current Constant Voltage
Communication	CAN

B. DC/DC converter characteristics

Figure 9(a) shows the converter efficiency of the input voltage. Its operation is steady compared with the input voltage change, though efficiency decreases by about 1% in the range of the boost mode compared with the buck mode. Even if the output voltage is changed, it has a similar characteristics.

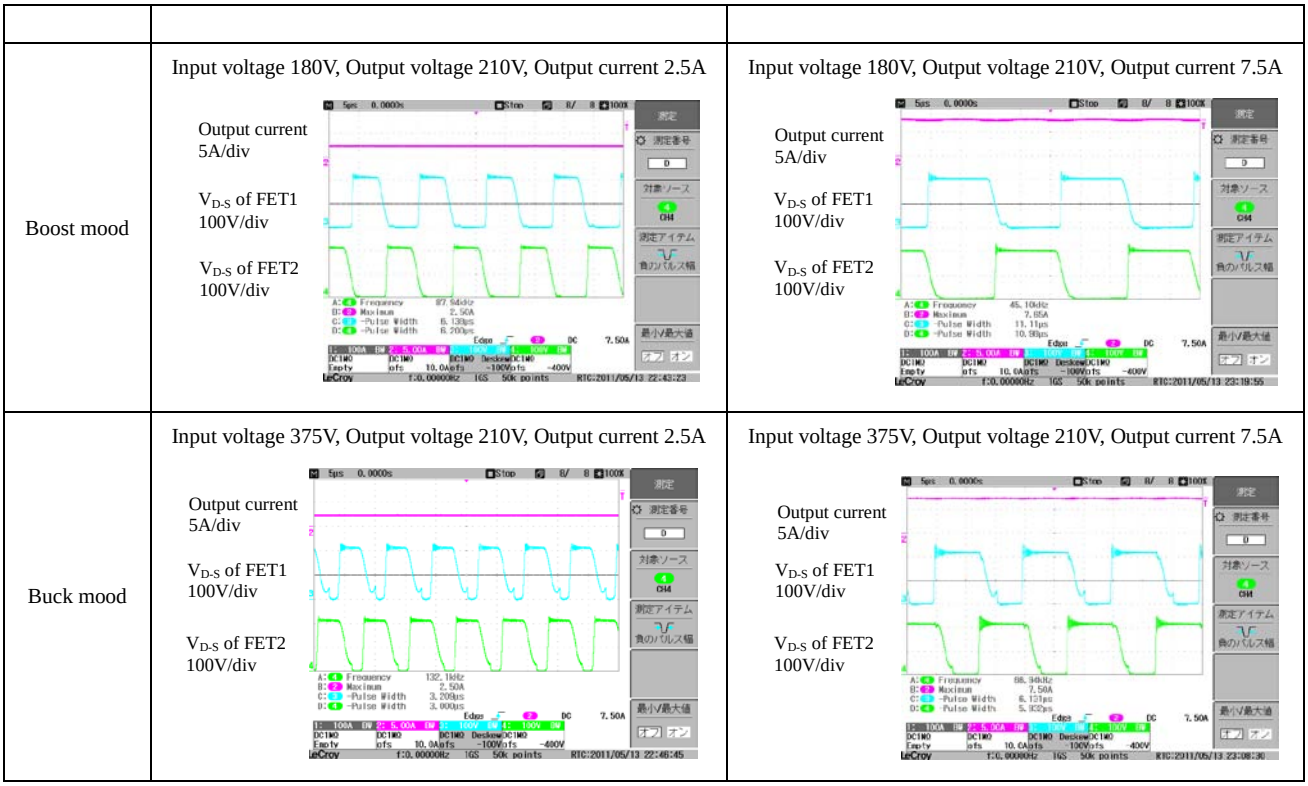

Fig. 8. Waveform DC/DC Convertor.

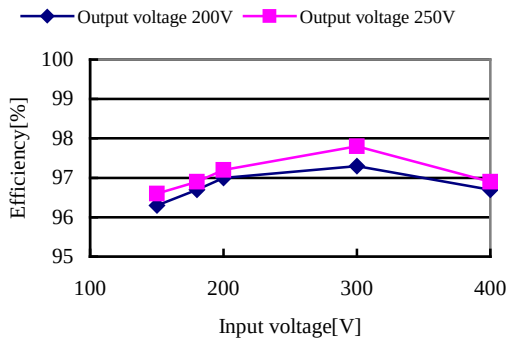

(a) Efficiency to the input voltage.

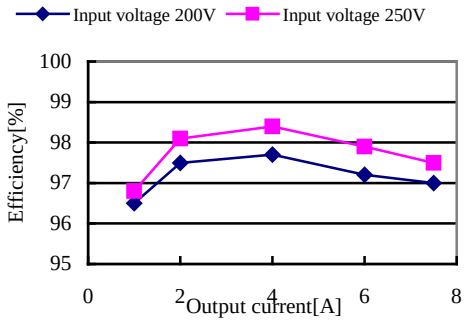

(b) Efficiency to the output current.

Fig 9. Characteristics of DC/DC convertor.

Figure 9(b) shows the converter efficiency to the output current . The efficiency at a light load decreases by 2% compared with the maximum efficiency.

It is shown by these characteristics that the proposed DC/DC converter can steadily control the charge.

C. Charge characteristics

The charge experiment was done using a battery in which 17 series were connected to a car battery (12V, 35Ah).

The experiment was changed at the same time by gap change from 30mm to 110mm and forward direction *x* change from 0mm to 45mm and lateral direction *y* from 0mm to 250mm.

The charge output characteristics are shown Figure 10(a) and the charge efficiency (P4/P1 of Figure 2) is shown in Figure 10(b). If it was a gap of 70mm, it could be charged at the rated power even with forward direction misalignment of 45mm and simultaneous lateral direction misalignment of 150mm, and the charge efficiency at this time was roughly 90%, as shown in Figure 10.

It was confirmed to charge highly effectively and stably, in these experiment results, and also when equipped to a PHEV.

D. Leakage flux density measurement

As for the contactless feeding power transformer, the leakage flux is generated by the loose coupling around the transformer.

Figure 11 shows the state for a gap of 70mm without misalignment, and the result of measuring the leakage flux density with 1.5kW feeding power while serving in the right and left of the vehicle and having swerved to create a 150mm gap and vehicles back and forth by 40mm. It is understood to become 6.25μT or less of the public exposure indicator of ICNIRP1998 if parting 850mm from the center of the transformer for a normal position with a gap of 70mm.

The leakage flux density when installing it from PHEV trunk bottom and a rear bumper at the position at 700mm became 14.5μT in a rear bumper. It is being eased by 27μT in the new standard for ICNIRP2010, and it seems that the standard can be cleared for the outside of the vehicle.

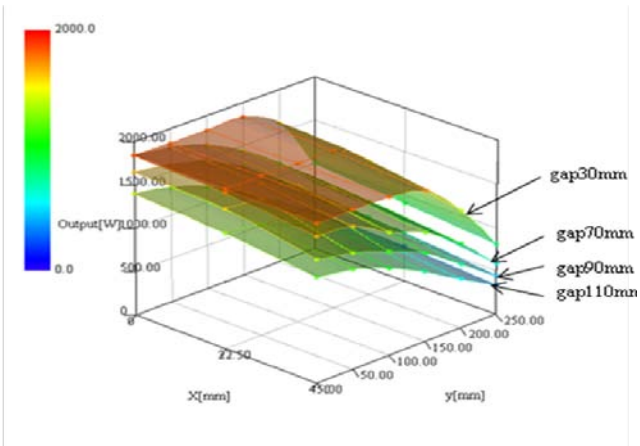

(a)Output power

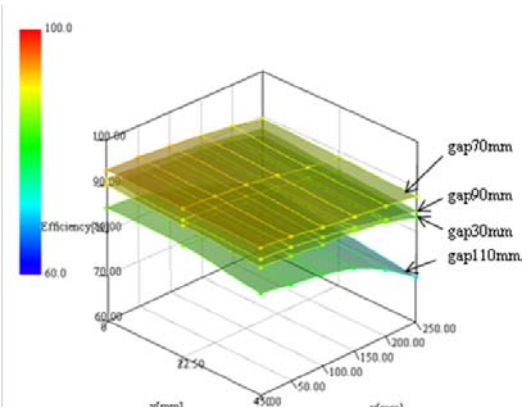

(b)Efficiency

Fig 10. Charastritics of contactless charging system .

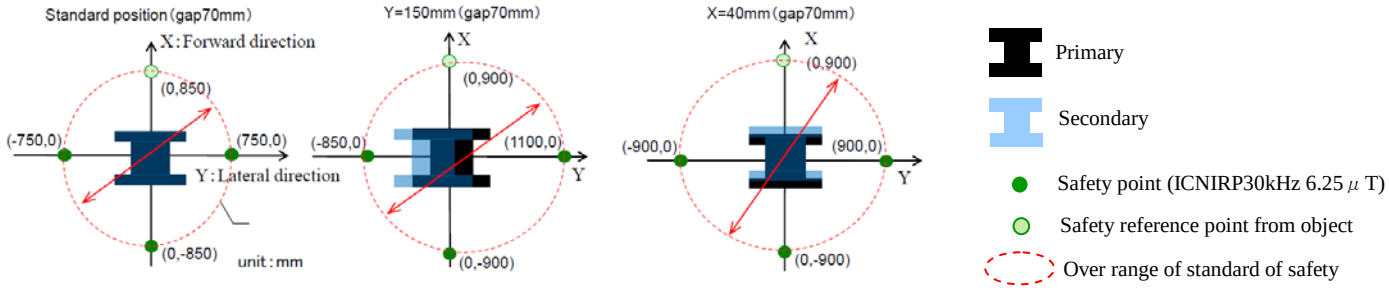

Fig 11. Leakage flux measurment result.

V. CONCLUSION

A double-sided winding transformer of a new core architecture (H–shaped cores) is proposed in this paper, and it was shown more efficient, more robust to misalignment and lighter compared with previous rectangular core.

Moreover, it shows development of a critical mode fly backing interleave DC/DC converter with buck-boost function, which charges highly effectively and stably, despite gap change and misalignment. The characteristics shown in this thesis are confirmed, and the authors think, that by equipping PHEVs with the system, these technologies will accelerate practical use of the contactless charging system.

ACKNOWLEDGMENT

This research was sponsored by the New Energy and Industrial Technology Development Organization (NEDO) of Japan. I wish to express my deep gratitude to all of the related people.

Moreover, we wish to express our gratitude to Y. Nagatsuka and M. Chigira of the Saitama University graduate school, who cooperated in the present study.

REFERENCE

(1) Y. Kamiya, Y. Daisho, H. Mastuki, “Inductive Power Supply System for Electric-driven Vehicle.” JIEEJ, Vol. 128, No. 128, pp. 804-807, 2008

(2) M. Budhia, G.A. Covic and J.T Boys, “Design and Optimisation of Magnetic Structures for Lumped Inductive Power Transfer Systems", ECCE 2009 IEEE, pp. 2081-2088, 2009

(3) T. Yasuda, K. Ida, S. Abe, Yasuyoshi Kaneko, A. Suzuki, Yamanouchi, "Noncontact charging system (the second report)", 2011 JSAE Annual Congress (Autumn), 261-20105612 , 2010

(4) N. Ehara, T. Iwata, Y. Kaneko, S. Abe, T. Yasuda, K. Ida "Characteristics comparison by noncontact feeding power transformer winding method for electric vehicle", IEEJ Transactions on Industry Applications, Japan, Vol. 130, No. 6, pp. 734-741 and 2010.

(5) Y. Nagatsuka, N. Ehara, Y. Kaneko, S. Abe and T. Yasuda: “Compact Contactless Power Transfer System for Electric Vehicles”, IPEC2010-Sapporo, pp. 807-813 (2010)

(6) Y. Nagatsuka, S. Noguchi, Y. Kaneko, S. Abe, T. Yasuda, K. Ida, A. Suzuki, and R. Yamanouchi: “Contactless Power Transfer System for Electric Vehicle Battery Charger", EVS-25 Shenzhen, China, 2010

(7) G.A. Covic, J.T. Boys, M. Budhia and C.Y. Huang: “Electric Vehicles-Personal transportation for the future", EVS-25 Shenzhen, China, 2010

(8) M. Budhia, G.A. Covic, and J.T. Boys “A New Magnetic Coupler for Inductive Power Transfer Electric Vehicle Charging Systems”, IECON 2010 IEEE, pp. 2481-2486, 2010